Biomed Microdevices (2012) 14:95–107
DOI 10.1007/s10544-011-9588-5

Fabrication of cell container arrays with overlaid surface topographies

Roman Truckenmüller · Stefan Giselbrecht · Maryana Escalante-Marun · Max Groenendijk · Bernke Papenburg · Nicolas Rivron · Hemant Unadkat · Volker Saile · Vinod Subramaniam · Albert van den Berg · Clemens van Blitterswijk · Matthias Wessling · Jan de Boer · Dimitrios Stamatialis

Published online: 3 November 2011

Abstract This paper presents cell culture substrates in the form of microcontainer arrays with overlaid surface topographies, and a technology for their fabrication. The new fabrication technology is based on microscale thermoforming of thin polymer films whose surfaces are topographically prepatterned on a micro- or nanoscale. For microthermoforming, we apply a new process on the basis of temporary back moulding of polymer films and use the novel concept of a perforated-sheet-like mould. Thermal micro- or nanoimprinting is applied for prepatterning. The novel cell container arrays are fabricated from polylactic acid (PLA) films. The thin-walled microcontainer structures have the shape of a spherical calotte merging into a hexagonal shape at their upper circumferential edges. In the arrays, the cell containers are arranged densely packed in honeycomb fashion. The inner surfaces of the highly curved container walls are provided with various topographical micro- and nanopatterns. For a first validation of the microcontainer arrays as *in vitro* cell culture substrates, C2C12 mouse premyoblasts are cultured in containers with microgrooved surfaces and shown to align

Roman Truckenmüller and Stefan Giselbrecht contributed equally to this paper

Electronic supplementary material The online version of this article (doi:10.1007/s10544-011-9588-5) contains supplementary material, which is available to authorized users.

R. Truckenmüller (✉) · N. Rivron · H. Unadkat · C. van Blitterswijk · J. de Boer
MIRA Institute for Biomedical Technology and Technical Medicine, Department of Tissue Regeneration, University of Twente, Drienerlolaan 5, 7522 NB Enschede, The Netherlands
e-mail: r.k.truckenmuller@utwente.nl

B. Papenburg · M. Wessling · D. Stamatialis
MIRA, Membrane Science and Technology, University of Twente, Drienerlolaan 5, 7522 NB Enschede, The Netherlands

A. van den Berg
MESA+Institute for Nanotechnology, BIOS, The Lab-on-a-Chip Group, University of Twente, Hallenweg 15, 7522 NH Enschede, The Netherlands

M. Escalante-Marun · V. Subramaniam
MESA+, Biophysical Engineering, University of Twente, Drienerlolaan 5, 7522 NB Enschede, The Netherlands

S. Giselbrecht
Karlsruhe Institute of Technology, Institute for Biological Interfaces, Hermann-von-Helmholtz-Platz 1, 76344 Eggenstein-Leopoldshafen, Germany

V. Saile
Karlsruhe Institute of Technology, Institute for Microstructure Technology, Kaiserstraße 12, 76131 Karlsruhe, Germany

M. Groenendijk
Lightmotif B.V., Pantheon 12, 7521 PR Enschede, The Netherlands

along the grooves in the three-dimensional film substrates. In future stem-cell-biological and tissue engineering applications, microcontainers fabricated using the proposed technology may act as geometrically defined artificial microenvironments or niches.

Keywords Microwell arrays · Polymer films · Polylactic acid (PLA) · Nanoimprint · Thermoforming · Tissue engineering

1 Introduction

1.1 Motivation and state of the art

The fate of cells adhering to the surfaces of cell culture substrates or tissue engineering (TE) scaffolds is closely related to the properties of the substrates themselves. These include not only the biophysicochemical or material properties of the substrate surfaces, but also their geometrical or morphological properties. For many years now, numerous studies have revealed the influence of surface morphology of culture substrates on various cell- and tissue-physiological aspects (Curtis and Clark 1990; Curtis and Wilkinson 1997; Flemming et al. 1999; Martinez et al. 2009; von Recum and van Kooten 1995; Singhvi et al. 1994). This covers the influence of engineered micro- and nanotopographies on cell adhesion, morphology, orientation, migration, viability, proliferation, gene expression or differentiation. A classical study is on the behaviour of cells cultivated on surfaces with step (Clark et al. 1987) or groove and ridge patterns (Clark et al. 1990; Walboomers and Jansen 2001). An easy-to-read-out indicator for cell-surface-topography interactions in this case can be the alignment of elongated cells along the underlying pattern, a phenomenon which is referred to as 'contact guidance' (Weiss 1958; Zhou et al. 2009).

To create well-defined surface topographies on a cellular and subcellular scale, in the above-mentioned studies, a variety of micro- and nanotechnologies was applied (Flemming et al. 1999; Hasirci and Kenar 2006). The substrates or their coatings were from many different materials such as quartz, titanium or diverse polymers, among others also biodegradable ones as polycaprolactone (PCL) or polylactic acid (PLA). Topographical features such as grooves, wells, pits or pillars were generated mainly by all kinds of lithographic processes, typically as direct lithography or followed by subtractive pattern transfer via etching. Topographies were also generated by polymer moulding using templates prepared by means of the lithographic processes mentioned before.

The past studies on interactions of cells and surface topographies created by lithographical means were performed on planar substrates. However, cells *in vivo* often experience three-dimensional (3D), spatially curved interfaces. From a certain small radius of curvature on, curved surfaces can be sensed as such by cells adhering to them. Already in the 1960's, it was found that fibroblasts grown on cylindrical glass fibres with diameters less than 100 μm elongate and align with the fibres (Curtis and Varde 1964). In a recent study, L929 mouse fibroblasts and human mesenchymal stem cells (hMSCs) were cultured in and on concave and convex spherical calottes from polydimethylsiloxane (PDMS) with a diameter of 200–300 μm, and a depth or height of 50–150 μm (Park et al. 2009). This study clearly indicates that cells sense and respond to microscale surface curvatures. The cells escaped from the concave calottes whereas they did not from the convex ones. Therefore, providing topographies on curved instead of planar substrates seems to be highly relevant, and that not only for cell-biological *in vitro* studies in academia. Findings from such studies may later be transferred to scaffolds for clinical TE applications. But while lithographic patterning even on a nanoscale is comparatively easy to perform on planar substrates, it is difficult on curved 3D substrates. This is especially true for small curvature radii in the hundred micrometres range, for example.

1.2 New approach

To provide against this background even highly curved cell culture substrates with surface topographies, the present paper takes a new approach for micro- and nanopatterning. We chose a thin thermoplastic polymer film as our substrate and thermal moulding for its topographical patterning. This material and process choice enables a potential future fabrication of topographically patterned culture substrates on an industrial scale. In the new approach, patterning is not performed on a curved substrate, but, in a first step, still on a planar substrate. To then end up with a patterned 3D substrate, in a second step, the prepatterned planar substrate is formed to the corresponding shape, and that in such a way that its topographical surface patterns are preserved. For this, the film is not heated to a liquid or flowing state, but only to a softened, still solid state of the polymer. Thus, the heated polymer film is formed under conditions of high material coherence. This is called 'thermoforming' (Throne 1996), which can be defined as shaping of heated semi-finished products in the form of thermoplastic films or plates, with their edges fixed, by three-dimensional stretching.

In this paper, we present 3D substrates in the form of microcontainer arrays with overlaid surface topographies, and a technology for their fabrication. According to the above approach for providing curved substrates with topographical patterns, the new fabrication technology is based on microscale thermoforming of thin polymer films whose surfaces are prepatterned by thermal micro- or nanoimprinting. This approach was first suggested by the joint first authors of the present paper in the framework of a previous paper in this journal. They did this after they recognised that stochastic

topographies on the surface, or surface roughness, of a flat film could be found again on the film after thermoforming it, even if distorted (Giselbrecht et al. 2006). Now, the authors present new experimental data proving the feasibility of their former idea. For microthermoforming, we applied a new process on the basis of temporary back moulding of polymer films. The novel cell container arrays were fabricated from PLA films. The thin-walled microcontainer structures have the shape of a spherical calotte. Their highly curved walls were provided with various topographical micro- and nanopatterns, among others with groove patterns. For a first validation of the 3D film substrates' ability to affect cells via the topographies on their curved surfaces, we performed a contact guidance experiment using C2C12 mouse premyoblasts. The idea is that in future stem-cell-biological and TE applications microcontainers fabricated using the proposed technology may act as geometrically defined microenvironments or niches for single cells, cell layers or cell aggregates. These artificial environments could then, for instance, allow to engineer microtissues as relevant 3D *in vitro* models in pharmaceutical and toxicological research.

2 Materials and methods

2.1 Fabrication of cell container arrays

2.1.1 Microthermoforming by temporary back moulding

For microthermoforming, so far, we applied an adaptation of macroscopic 'pressure forming' (Throne 1996) where compressed nitrogen was used to force thin polymer films into the cavities of micromoulds (Giselbrecht et al. 2006; Truckenmüller et al. 2002; Truckenmüller et al. 2008). Now, a new process based on temporary back moulding of polymer films was applied. The microscale back moulding process was carried out in a simple hot press (Fontune, Holland; with water cooling). To perform the new process (Fig. 1(a)–(d)), a stack of sheets and films is inserted between the press plates. The stack consists of a two-part mould from metal sheets, a first, thin thermoplastic film to be thermoformed and a second, thicker (stack of) thermoplastic film(s) for back moulding the first film. The first film is sandwiched between the mould and the second film. If possible, the second film is chosen in such a way that if the first film is in a softened state best suited for thermoforming, at the same temperature, the second film is in a softer or even liquid state well-suited for hot embossing. After insertion of the mould and film stack, the press is closed to such an extent that the stack is not yet clamped between the press plates (Fig. 1(a)). Then the press is heated up. Around the softening temperature of the polymer of the first film, the press is closed such that the first film is formed into the microcavities of the mould by the pressurised, softened or flowing polymer of the second film to the desired extent (Fig. 1(b)). Next, the press is cooled down.

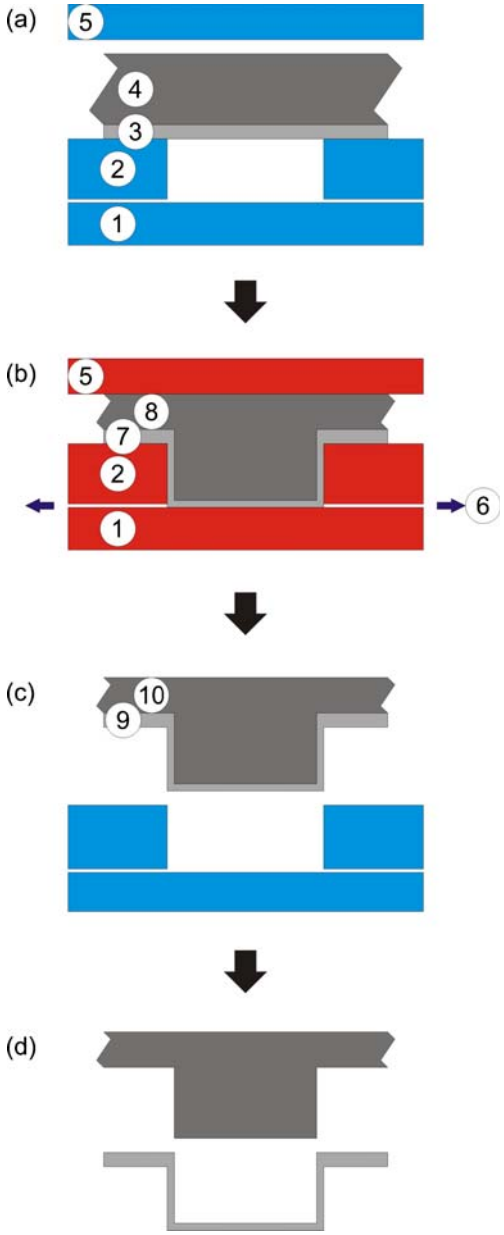

Fig. 1 Process for microthermoforming based on temporary back moulding with the following process steps: insertion of a stack of mould sheets and polymer films, (**a**) closing the press without clamping the stack, heating up the press, (**b**) back moulding the film to be thermoformed by pressing, cooling down the press, opening the press, unloading the stack, (**c**) demoulding the thermoformed and back-moulded film, and (**d**) peeling off the thermoformed film microstructure (simplified scheme with only a single mould cavity; film fully formed into the cavity; (1) mould support, (2) micromould, (3) thermoplastic film, (4) thicker thermoplastic film with lower softening temperature, (5) upper press plate, (6) displaced air, (7) softened and formed film, (8) compressed softened or flowing polymer, (9) solidified thermoformed film substrate, (10) solidified backing; for ((1), (2) and (5)): blue or mid grey and red or dark grey corresponds to cold and heated)

After that, the pressure is released and the press is opened. Then the stack is unloaded and the thermoformed and back-filled film is demoulded (Fig. 1(c)). Finally, the thermoformed

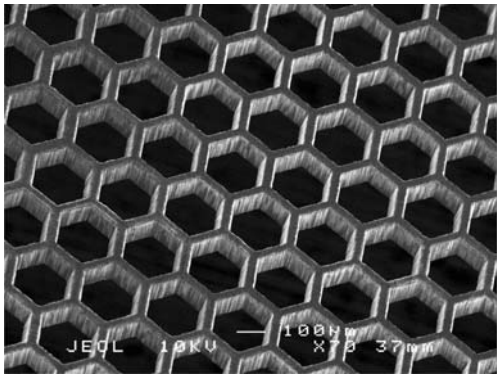

Fig. 2 Section of the perforated-sheet-like micromould from stainless steel for thermoforming the cell container array (SEM image; tilted view; mean incircle diameter of the hexagonal through holes, or clearance of the honeycomb mesh: 220 μm; mean web width: 30 μm; through hole length, or thickness of the metal sheet: 100 μm)

film is separated from its embossed backing just by peeling off the film (Fig. 1(d)) or by selectively dissolving or etching the backing. For the fabrication of the microcontainer arrays, we chose the peeling method.

Until now, for microthermoforming, a one-piece mould in the form of a thicker metal plate with blind-hole-like micro mould cavities was used (Truckenmüller and Giselbrecht 2004; Truckenmüller et al. 2008). Now, as mentioned above, we used a novel two-piece mould. It consists of the mould itself in the form of a thinner metal sheet with through holes representing the sidewalls of the mould cavities, and of an underlying mould support, also in the form of a sheet, representing the cavity bottoms (Fig. 1). The support can coincide with the lower plate of the hot press. The perforated-sheet-like mould (Fig. 2) and its support were made of 100 μm thick sheets from high-grade steel (X5 CrNi 18 9; RECORD Metall-Folien). The through holes were hexagonal holes and arranged densely packed in honeycomb fashion. They were fabricated by laser micromachining. For the laser ablation, a femtosecond pulsed titanium sapphire laser was used (Coherent; central wavelength: 800 nm; pulse repetition rate: 50 kHz; pulse energy: 5 μJ; settings: 200 fs pulse length, circular polarisation, 25 μm laser spot diameter). The through holes were fabricated with sidewall slopes of approximately 5° to facilitate, in the form of draft angles, demoulding of the thermoformed film substrates.

For the fabrication of the cell container arrays, we chose a semi-finished product in the form of a FDA (U.S. Food and Drug Administration) compliant, 35 μm thin film (nominal thickness: 30 μm) from a blend of PLA (Plastic Suppliers/Sidaplax; EarthFirst Packaging Film, PF; blown film, biaxially oriented; glass transition temperature: 58°C; melting temperature: approximately 160°C; surface tension of untreated surface: 38 mN m^{-1}). An approximately 500 μm thick stack of polyethylene (PE) films cut out from zip-lock plastic film bags (Overtoom) was used for back moulding the PLA film.

2.1.2 Surface texturing by overlaid thermal imprinting

Providing the inner surfaces of the highly curved walls of the cell container arrays with topographical micro- and nanopatterns was achieved by a new combination of thermal imprinting or hot embossing, and microthermoforming (Fig. 3(a) and (b)). For this, first a polymer film substrate is patterned by micro- or nanoimprinting (Fig. 3(a)). Then the prepatterned substrate is thermoformed by microscale back moulding with the topographical pattern being preserved (Fig. 3(b)).

Imprinting was carried out in a dedicated machine for hot embossing nanoimprint lithography (NIL; Obducat; NIL 6") as well as in a simple conventional hot press (Specac; with water cooling). To perform the imprinting process, in case of the NIL machine, an imprinting stamp from silicon and the PLA film to be imprinted were inserted between the substrate plate and the sealing foil separating the vacuum section of the machine from its high-pressure section (Obducat; Poly-foils). The PLA film was sandwiched between the stamp and the sealing film. At the end of the imprinting process, the delicate imprinted film was peeled from the stamp together with the stiffer sealing foil. Thus, the risk of overstretching the film during demoulding was reduced.

The stamps carried periodical patterns of parallel micro- or nanoridges (Table 1), and circular and triangular micropillars and -pits. The stamps which carried the micropatterns were fabricated by standard photolithography followed by reactive ion etching. The stamp carrying the nanopattern was fabricated by laser interference lithography and wet chemical etching (Haneveld 2006). To facilitate demoulding, the

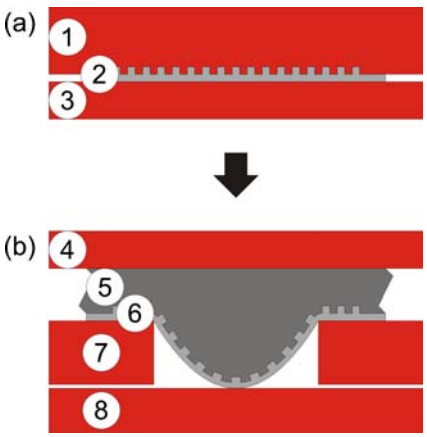

Fig. 3 Process for the generation of micro- and nanotopographies on the surfaces of 3D film substrates by an overlay of microthermoforming and thermal imprinting with the following two main process steps: (**a**) micro- or nanoimprinting and (**b**) thermoforming by micro back moulding (simplified scheme; (1) imprint stamp, (2) imprinted thermoplastic film, (3) film support, (4) upper press plate, (5) compressed softened or flowing polymer, (6) imprinted and thermoformed film, ((7) and (8)) thermoforming mould)

Table 1 Micro- and nanogroove patterns on the stamps/imprinted films

Ridge/groove width	Pattern periodicity	Pattern height/depth	
3.5 μm	15 μm	3 μm	[a]
1.5 μm	8 μm	3 μm	[a,b]
5 μm	15 μm	500 nm	
3 μm	8 μm	500 nm	
150 nm	500 nm	100 nm	

[a] Micropattern chosen for the cell culture experiment. [b] See Fig. 8

stamps were functionalised with a perfluorodecyltrichlorosilane (FDTS; ABCR) anti-stiction layer by vapour deposition.

To perform now the thermoforming and imprinting overlay, the micro- or nanopatterned films were introduced into the back-moulding-based microthermoforming process. Due to the fact that the periodicities of the groove patterns were more than one order smaller than the container structures, alignment of the imprinted patterns with the hexagonal through holes of the mould could be restricted to adjusting the longitudinal axes of the grooves parallel to major axes of the hexagonal holes. This could be carried out without any technical aid such as a microscope or a micromanipulator, just by eye and by hand. To achieve a high replication accuracy of the moulded patterns in the imprinting step and to thermally fix the imprinted patterns to a great extent, the moulding temperature should be chosen to be comparatively high. However, maintaining the initial defined thickness and low thickness deviations of the semi-finished product over the imprinted area is easier at lower imprinting temperatures. A defined, equal thickness of the non-imprinted and of the imprinted films to be thermoformed is essential due to the fact that, as generally in thermoforming, the semi-finished product thickness has a direct impact on the final part geometry. To then preserve the imprint patterns to a greater extent in the subsequent microthermoforming step, the forming temperature should be relatively low, and lower than the imprint temperature. Concerning the found temperatures, see section 3.1.

2.2 Cell culture experiment

2.2.1 Introductory remarks

For a first validation of the microcontainer arrays as *in vitro* cell culture substrates and the 3D film substrates' ability to affect cells in a controlled manner via the topographies on their curved surfaces, we performed a contact guidance experiment. For this, cells of the C2C12 mouse premyoblast cell line (American Type Culture Collection, ATCC number CRL-1772) were cultured in microcontainers with grooved surfaces. C2C12 cells were chosen as they already proved themselves in contact guidance experiments on planar substrates (Charest et al. 2007; Papenburg et al. 2007). It was then checked if the groove patterns on the cell container walls allow cell alignment. This was done in view of the fact that the patterns belong to substrates which, along with thermoforming, underwent a three-dimensional stretching and which, as a consequence thereof, were not only spatially curved, but also distorted. For the cell culture trials, we chose substrates thermoformed from films which were imprinted using the stamps with the coarser and the finer 3 μm high micropattern (Table 1; first and second row, respectively). Besides the films with both the microcontainer structures and one of the two microgroove patterns, as negative controls, we applied films with only the microcontainer structures. Additionally to the three types of curved substrates, to verify the contact guidance capacity of the microgroove patterns in combination with C2C12 cells in principle, three planar substrate types were applied. These were films with only one of the two microgroove patterns and unprocessed films without microcontainer structures and microgroove patterns, the latter again as negative controls. The microcontainer arrays in the films comprised approximately 1200 containers in a circular area of approximately 8 mm diameter. The cell culture was performed in a 24-well plate (Nunc; multidish, Nunclon Delta SI).

2.2.2 Preparative work

For this, circular samples were punched out from the micropatterned and -structured films. Having a diameter of 15 mm, the film samples fitted exactly into the wells. Then the samples were cleaned by immersing them in ethanol for 30 min and allowing the ethanol to evaporate. Next, the films were mounted into the well plate. O-ring seals (ERIKS; compound Viton 75 51414; size 14×1 mm) were used to secure them at the well bottoms. After that, the samples and the well plate were sterilised by spraying them with a 70% isopropanol solution and allowing the solution to evaporate. Then the films in the wells were incubated in phosphate-buffered saline (PBS) at 37°C for 1 day.

2.2.3 Culturing

For cell cultivation, 1 ml cell culture medium was centrifuged into each sample-loaded well at 3184 rcf for 40 s and aspirated. The culture medium used was C2C12 proliferation medium composed of Dulbecco's Modified Eagle's Medium (DMEM; Gibco) supplemented with 10% (v/v) foetal bovine serum (FBS; Lonza), 100 U ml^{-1} penicillin (Gibco) and 100 μg ml^{-1} streptomycin (Gibco). Then C2C12 cells were trypsinised from a cell culture flask. Next, 1 ml suspension of cells and medium with a concentration of 20,000 cells ml^{-1} was centrifuged into each well at 300 rcf for 4 min resulting in a mean seeding density of 10,000 cells cm^{-2}. Then the cell-seeded films were incubated at 37°C in a humidified atmosphere with 5% carbon dioxide for 2 days.

2.2.4 Fixation, staining and fluorescence microscope imaging

For cell fixation, the cells were first rinsed with PBS. Then they were fixed with a 4% paraformaldehyde solution for 10 min and rinsed with PBS. Next, the cells were permeabilised with a 0.1% (v/v) Triton X-100 (Sigma-Aldrich) solution for 4 min and rinsed with PBS. Finally, they were stained by incubating them in the dark in a 2.5% (v/v) Alexa Fluor 568 phalloidin (Molecular Probes) solution for 20 min and a 0.7 μg ml^{-1} DAPI (Sigma-Aldrich) solution for 10 min, and rinsed with PBS. For an evaluation of cell morphology concerning spreading and elongation, and of cell alignment, the fluorescently labelled cytoskeletons and nuclei of the cells were imaged using a fluorescence microscope (BD Biosciences; Pathway 435).

2.2.5 Quantification

For a quantitative evaluation of cell alignment in case of the microcontainer structures with and without the overlaid microgroove patterns, the images were analysed using image processing and analysis software (ImageJ, version 1.43). As in previous studies on planar, uncurved groove patterns (Charest et al. 2004), cell alignment was quantified by measuring the orientation angle of the major axes of the cell bodies, axes which would result from fitting the cells with ellipses, with respect to the longitudinal axes of the microgrooves. The cells considered for the angle measurements were cells in the concave cell containers, not on the convex ridges between the containers and, for technical reasons, not on the smaller steep parts of the curved container walls. To be able to compare the results of the angle measurements and to convert them into a graphical representation in the form of a bar graph, the continuous orientation angle range ±(0–90°) was subdivided into the nine equal discrete ranges ±(0–10°), ±(10–20°), ±(20–30°), … and ±(80–90°).

2.2.6 Statistics

For all six film types, the cell culture experiment was performed in triplicates, that is in each case using three film samples in three independent wells. For the quantification of cell alignment in case of the three curved substrate types, 50 cells per sample or well were measured. To verify the significance of measurement results, the Student's *t*-test was applied. Results were considered to be significantly different from each other for *p*-values smaller than 0.05.

2.2.7 Dehydration, critical point drying and SEM imaging

For dehydration, the cells were rinsed with PBS first. Then they were dehydrated by immersing them in a 50, 60, 70, 80, 90, 96 and 100% ethanol solution for 15 min each. Next, the cells were dried in a critical point dryer (Balzers; CPD 030). Finally, the cells including the film samples were coated with gold in a sputter coater (Cressington; 108auto). For a qualitative evaluation of cell alignment, the cells were imaged using a scanning electron microscope (SEM; Philips/FEI; XL30 ESEM-FEG).

3 Results and discussion

3.1 Fabrication of microcontainer arrays

3.1.1 Micro back moulding

Thermoforming of the PLA film by temporarily back moulding it with the material of the PE film stack was performed at a forming temperature of 82°C and a mean forming pressure of approximately 10 MPa. In view of the thermomechanical properties of the PLA film, the forming temperature could have been lower. With a view to the PE films, however, the temperature had to be chosen such that,

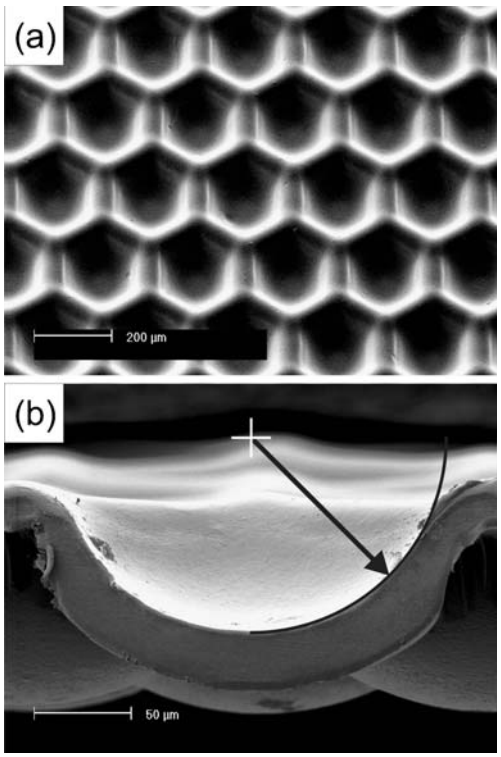

Fig. 4 Microcontainers of a PLA cell container array without micro- or nanopatterns on the inner surfaces of their walls (SEM images; (**a**) tilted top and (**b**) cross-sectional view; periodicity of the containers within the arrays: 250 μm; incircle diameter of the hexagonal containers at half inner container depth: approximately 170 μm; maximum inner container depth: approximately 100 μm; mean wall thickness of the containers: approximately 30 μm; arrow in (**b**) represents inner curvature radius of the containers of approximately 100 μm)

Table 2 Tested combinations for micro back moulding

Film to be thermoformed	Film for back moulding	Method for separating the thermoformed film from its backing
30 μm thin PLA[a]	PE	Peeling off [b]
25 μm thin PP[a,c]	PE	Peeling off
20 μm thin PC[d]	PP	Peeling off
25 μm thin PP[a]	PMMA[e]	Dissolving in acetone
20 μm thin PC	PMMA	Dissolving in 70% isopropanol

[a] Biaxially oriented. [b] Combination chosen for the cell container array. [c] Polypropylene. [d] Polycarbonate. [e] Polymethylmethacrylate

for finite pressures, the shear modulus of the PE material allowed a defined back filling. This was the case for a temperature of approximately 82°C and higher. The dwell time between reaching the forming pressure and the beginning of the cooling was practically zero. The pressure release was performed near room temperature. Using these forming parameters, in a kind of free forming variant of the back moulding process, the PLA film touched the cavity bottoms of the mould just in their centres. As a consequence, the film in each case adapted the shape of a spherical calotte (Fig. 4(a) and (b)). The curvature radius of this cap was approximately 100 μm (Fig. 4(b)) and therefore in the same range as the curvature radii of the PDMS calottes sensed by L929 cells and hMSCs in the study mentioned in the section 1.1 (Park et al. 2009). Due to the guidance by the mould, the shape of the free-formed spherical calotte merged into a hexagonal shape at the upper circumferential edges of the containers (Fig. 4 (a)). For suitably higher forming temperatures or pressures, for example for 85°C and 15 MPa, it is in principle also possible to force the film to precisely adapt the shape of the mould cavities resulting in flat bottoms of the cell containers (supplementary material, Fig. S1). However, such microstructures were only fabricated for demonstration purposes and not used in the cell culture experiment.

Besides the combination of PLA and PE for the film to be thermoformed and the film for back moulding, respectively, other film combinations were successfully tested, too (Table 2). In these tests, the thermoformed film was separated from the backing not only by peeling off the film, but also by dissolving the backing.

For the new micro back moulding process, in contrast to the micro pressure forming process applied so far, it is not necessary to provide equipment for gas pressurisation and to integrate it into the moulding press or tool. Closely related is another advantage of the new process. The back-moulding-based microthermoforming process easily allows to safely apply very high forming pressures. In micro back moulding, the pressure medium in the form of a nearly incompressible polymer melt is pressurised inside the thermoforming mould. This is in contrast to micro pressure forming with highly compressed gas as pressure medium, also outside the tool, for instance in a supply line. The benefits of higher pressures are that they enable higher forming accuracies concerning mould replication and lower forming temperatures. The latter is important when forming films with temperature sensitive topographical (this paper) or other premodifications (Giselbrecht et al. 2006; Gottwald et al. 2007; Truckenmüller et al. 2008). The new microthermoforming process provides further technology and application-technological advantages and options. Besides its high potential for high-throughput manufacturing, this includes handling advantages in case the backing is not removed directly after thermoforming, but remains for some time on the thermoformed film. Such a more stable, one-side plane carrier or protection can facilitate transport, intermediate storage, dicing, bonding or other postprocessing of the formed film.

In contrast to the downwardly closed microcavities of the conventional moulds used for microthermoforming up to now, the microcavities of the new perforated-sheet-like mould do not have to be evacuated every time when entering the thermoforming cycle. That means that vacuum equipment is unnecessary. This is because the air which is displaced by the

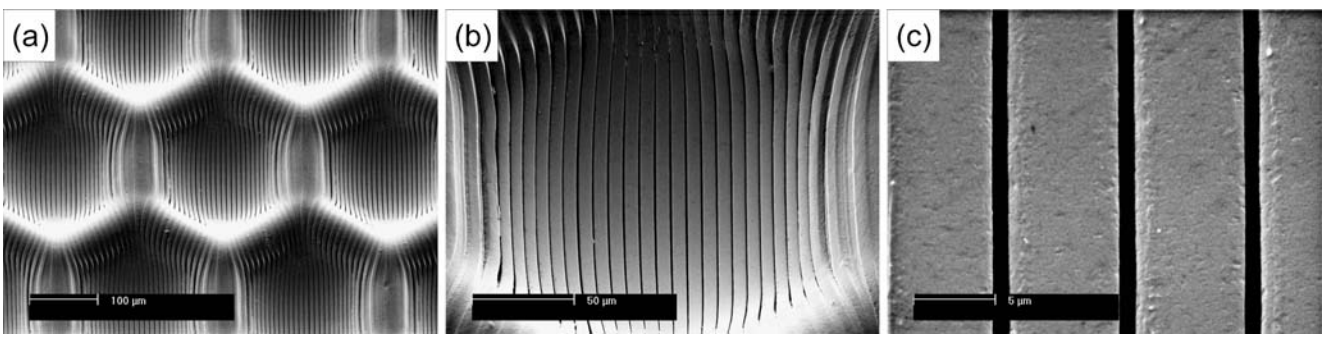

Fig. 5 (Sections of) Microcontainers of a PLA cell container array with a microgroove pattern on the inner surfaces of their walls, formed from a film such as the one shown in Fig. 8 (SEM images; tilted views; container dimensions: see caption of Fig. 4; groove width, periodicity and depth of the pattern on the PLA film prior to thermoforming: 1.5, 8 and 3 μm, respectively; ((**b**) and (**c**)) close-up views of the middle of (**a**))

film being formed into the cavities can escape through an implicit or explicit microgap between the mould and its support (Fig. 1(b)). To provide for such a gap, the surface of the mould sheet facing the support should be microrough or -textured. Another advantage of the new mould concept is the much smaller thermal mass of the mould sheet compared to a conventional plate-type mould. This can lead to considerably reduced cycle times of the 'variotherm(al)' forming process. The above two advantages of the new mould concept make it much more compatible with potential future high-throughput processes in microthermoforming on the basis of 'roll-fed' processes (Throne 1996). In addition to the advantages in the application of the two-part mould, there are advantages in the mould fabrication, too. So, compared to conventional metal moulds with their blind-hole-like mould cavities fabricated by mechanical micromachining, for example, much less effort is needed to provide much more flat and smooth bottoms of the mould cavities. The fully accessible surface of the mould support can easily be mirror-finished, for instance. Flat and smooth bottoms of the mould cavities result in according bottoms of the thermoformed containers, which in turn result in an improved imaging through the container bottoms with inverted microscopes.

3.1.2 Imprint overlay

For the fabrication of the micro- and nanotextured PLA cell container arrays (Fig. 5(a)–(c), 6(a)–(c) and 7(a)–(h), and supplementary material, Fig. S2), using the NIL machine, imprinting was performed at a temperature of 80°C and a pressure of 5 MPa. The dwell time was 5 min. The pressure release was performed at 42°C. Using these parameters, we achieved a good replication fidelity in the imprinting process (Fig. 8) with the PLA films maintaining their thickness within the measurement accuracy of the employed thickness gauge (Mitutoyo; ID-C112B; range of measurement: 0.001–12.7 mm). Thermoforming of the imprinted films, as already before of the non-imprinted films, was performed at 82°C and 10 MPa. As mentioned in section 2.1.2, it is desirable to choose the forming temperature lower than the imprinting temperature. However, for the above reason, see previous section (3.1.1), this was not possible. Despite the form closure between the positive topographical patterns on the thermoformed film (Fig. 5(a)–(c)) and the corresponding negative patterns on the backing (Fig. 9), for all patterns, film and backing could be easily separated from each other. This is due to the structural flexibility of the thin film substrates.

Notwithstanding the relatively high forming temperature, the micropatterns (Fig. 5(a)–(c) and 7(a)–(h), and supplementary material, Fig. S2) and even the initially only 100 nm deep nanopattern (Fig. 6(a)–(c)) can be found again on the highly curved bottoms and sidewalls of the thermoformed microcontainers in good and satisfactory condition, respectively. The patterns are distorted in a regular manner, and that depending on the local film deformation within and between the containers. The distortions of the groove patterns, for example, can be broken down into distortions of the positions of the grooves or the distances between them, and distortions of the grooves themselves or their cross sections. At the upper circumferential edges of the containers and on top of the ridges between them, the distances between the grooves are increased, and the grooves are widened and flattened (Fig. 5(a)). Here, the film or its surface is stretched. This is in contrast to small areas in edges between the sidewall segments of the hexagonal containers. In these areas, the distances between the grooves are decreased and the grooves are narrowed. For the film substrates thermoformed

Fig. 7 Microcontainers of PLA cell container arrays with eight different micropatterns in the form of arrays of bigger and smaller circular and triangular pits and pillars on their walls (SEM images; container dimensions: see caption of Fig. 4; depth of the patterns prior to thermoforming: 3 μm) ▶

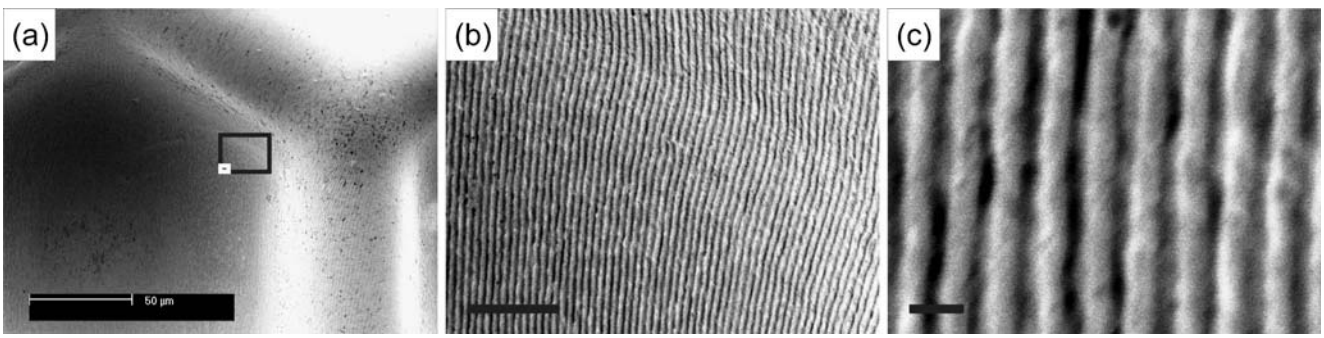

Fig. 6 Sections of a microcontainer of a PLA cell container array with a nanogroove pattern on its wall (SEM images; tilted views; container dimensions: see caption of Fig. 4; groove width, periodicity and depth prior to thermoforming: 150, 500 and 100 nm, respectively; black and white rectangle in (**a**) indicate the image section of the close-up views (**b**) and (**c**), respectively; scale bars represent (**b**) 5 μm and (**c**) 500 nm)

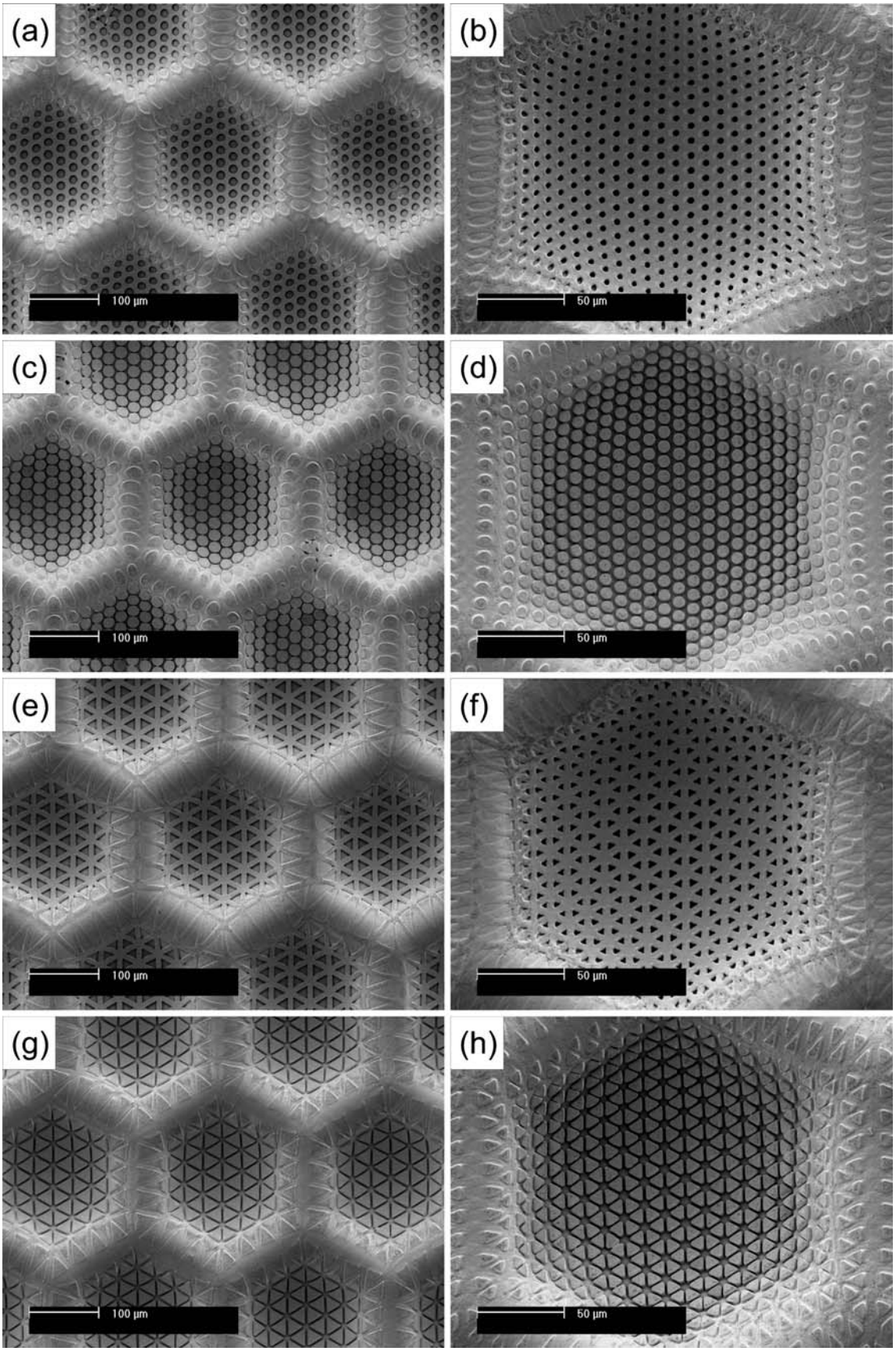
(a)
100 μm
(b)
50 μm
(c)
100 μm
(d)
50 μm
(e)
100 μm
(f)
50 μm
(g)
100 μm
(h)
50 μm

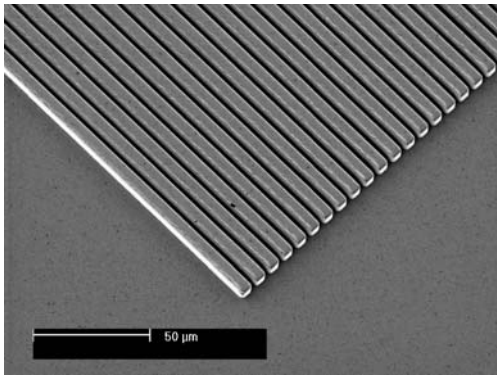

Fig. 8 Prepatterned PLA film (SEM image; tilted view; corner of patterned area; groove width, periodicity and depth: 1.5, 8 and 3 µm, respectively)

from the films with the 1.5 µm wide and 3 µm deep grooves, in these regions, the grooves are even narrowed to practically zero (Fig. 5(b); upper middle part). Here, the film surface is obviously compressed. However, with the distortions being highly reproducible, it should be possible to compensate distortions of the imprinted patterns during microthermoforming to a higher degree, at least laterally, by imprinting correspondingly predistorted patterns. This would then be comparable to macroscopic thermoforming of preprinted semi-finished products. Depending on the robustness of a certain cell-biological application to regular variations of distortions of a specific topographical pattern, for instance regarding periodicity variations, pattern predistortion can be omitted or achieved only by a single global mean distortion factor. A quantification of the pattern distortion due to the mechanics of film forming and the viscous nature of the polymeric pressurising medium, the latter causing friction and shear stress, has to be subject of further investigations. In this context, the impact of heating the imprinted film above its heat distortion temperature on the rounding of the edges of the imprinted patterns during thermoforming when there is no guidance by the imprint stamp has to be investigated, too. For the micropatterns, there is no substantial heat-induced edge rounding as can be seen by the sharp upper edges of the grooves in the area of the curved bottoms of the containers (Fig. 5(c)). In this area, the contribution of mechanical deformation on rounding of edges is obviously comparatively low, too. For the nanopattern on the thin PLA films, the extent of edge rounding is difficult to judge because the pattern is immediately destroyed by the electron beam of the SEM during imaging at correspondingly higher magnifications even at low acceleration voltages (Fig. 6(c)).

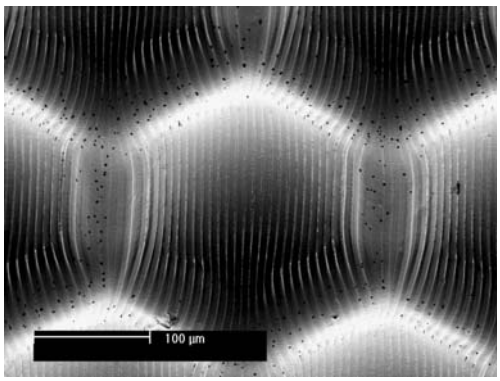

Fig. 9 PE backing with microridge surface pattern as it was peeled off from the film microstructure shown in Fig. 5 (SEM image; tilted view)

The approach for fabricating 3D substrates with overlaid surface topographies presented in this paper includes to keep the film substrate and to discard its backing. In principle, when not thin or flexible, but thicker or stiffer substrates are needed, it would be also possible to discard the film and stay with the backing. Another option is to copy the film or backing by electroplating or casting of an elastomeric resin. This copy could then be used as a 3D mould for thermoforming and simultaneously imprinting of flexible films or for soft embossing (Russo et al. 2002). That way, the cell culture substrates could be fabricated in a one-step moulding process instead, as described in the present paper, in two steps. Furthermore, a necessary alignment of the imprinted film to the thermoforming mould would be restricted to the mould fabrication.

3.2 Cell culture trials

3.2.1 Planar comparison substrates

The C2C12 cells adhere to and spread on all six types of PLA film substrates. This is indicated by propagated extensions of the mouse premyoblast cells or their elongation as a whole (Fig. 10(a)–(c), 11(a)–(c) and 12), both requiring attachment to the substrate.

On the unprocessed films without microcontainer structures and microgroove patterns, the cell bodies do not show a preferred orientation axis or angle (Fig. 10 (a)). In contrast, on the films with (only) the microgroove patterns, the preferred orientation axis of the cells is the longitudinal axis of the grooves, that is the cells are preferentially aligned along the grooves (Fig. 10(b) and (c)). This is true for the coarser microgroove pattern as well as for the finer one. These results are in good accordance with results from related studies with myoblasts on microgrooved planar substrates moulded from polymers. Said studies include C2C12 and primary mouse myoblasts on hot-embossed PC substrates (Charest et al. 2007) and C2C12 myoblasts on porous PLA substrates fabricated by phase separation micromoulding (Papenburg et al. 2007).

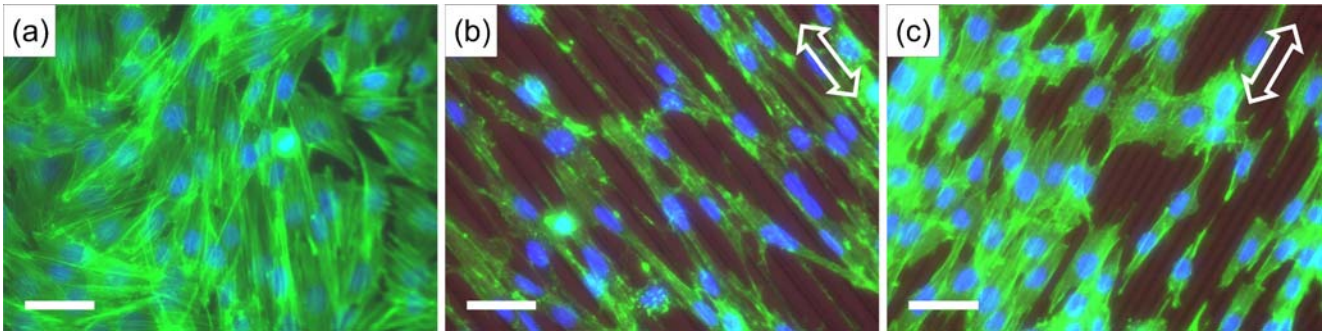

Fig. 10 C2C12 mouse premyoblast cells cultured for 2 days on planar substrates in the form of PLA films (**a**) without microgrooves and containers and ((**b**) and (**c**)) with only microgrooves (fluorescence microscope images; groove width, periodicity and depth: (**b**) 3.5, 15 and 3 μm, and (**c**) 1.5, 8 and 3 μm, respectively; fluorescent stained cytoskeletons and cell nuclei appear green and blue; double arrows highlight the direction of the planar groove patterns; scale bars represent 50 μm)

3.2.2 Curved substrates

On the films with (only) the microcontainers, the cell bodies show no preferred orientation (Fig. 11(a)). Regarding this, in case of the non-grooved surfaces, the cells on the curved substrates behave in a similar way as the cells on the planar substrates. In the theoretical case of a totally random and therefore uniform distribution of the cell orientation angle, in each of the nine orientation angle ranges, the cell count would be same, that is 100%/9≈11%. The mean (absolute value of the) cell orientation angle in this case would be 45°. Practically, the cell counts in the different angle ranges do not significantly differ from each other (Fig. 13; $p \geq 0.18$). The mean orientation angle is 42±1° and thus close to the theoretical value mentioned before. In contrast to that, on the films with both microcontainer structures and microgroove patterns, the cells are aligned along the grooves (Fig. 11(b) and (c)). This is true for cells on the curved bottoms as well as for cells on the curved sidewalls of the thermoformed containers (Fig. 12). Regarding cell alignment, now in case of the grooved surfaces, the cells on the curved substrates again behave in a similar way as the cells on the planar substrates. On the coarser microgroove pattern as well as on the finer one, the cell count in the angle range ±10° significantly differs from the count in all other angle ranges (Fig. 13; $p \leq 0.006$ and $p \leq 0.0068$, respectively). On the coarse pattern, 87±5% of the counted cells have an orientation angle in the range of ±10° whereas on the fine pattern, that is the case for 75±5% of the cells. Taken these numbers as a measure for alignment, as similarly suggested by other authors (also for cell nuclear alignment) (Charest et al. 2007; Clark et al. 1990), cell alignment is stronger for the coarse and weaker for the fine pattern. This trend is emphasised by the fact that the mean orientation angle of the cells on the coarse pattern is smaller than that of the cells on the fine pattern. The mean orientation angles are 6.3±0.5° and 13.2±0.6°, respectively. In the above-mentioned study on embossed planar substrates from PC, for a groove pattern with a groove width, periodicity and depth of 10, 20 and 5.1 μm, respectively, in case of C2C12 myoblasts, approximately 48% of the cell nuclei had an orientation angle in the range of ±10° (Charest et al. 2007). For the same pattern, now in case of primary myoblasts, approximately 77% of the

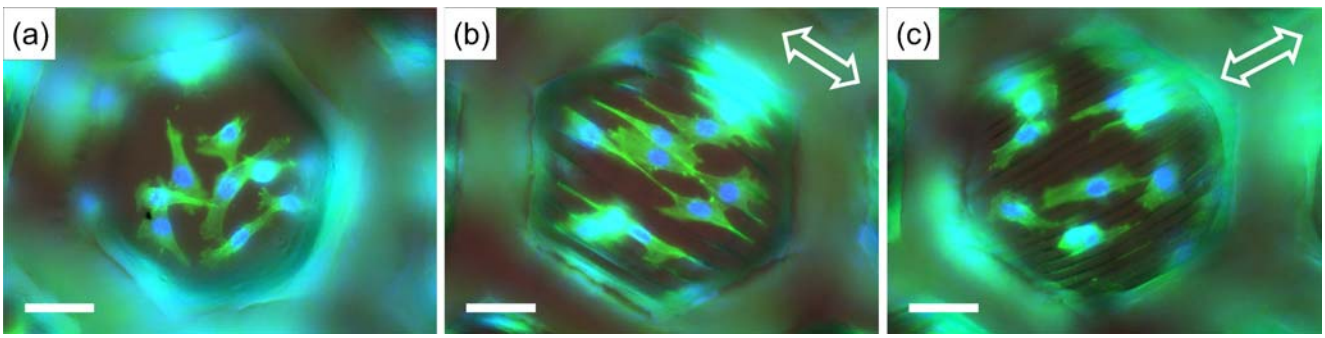

Fig. 11 C2C12 mouse premyoblast cells cultured for 2 days on curved substrates in the form of PLA films (**a**) with only microcontainers and ((**b**) and (**c**)) with both microgrooves and containers (fluorescence microscope images; groove width, periodicity and depth of the patterns on the PLA film prior to thermoforming: (**b**) 3.5, 15 and 3 μm, and (**c**) 1.5, 8 and 3 μm, respectively; fluorescent stained cytoskeletons and cell nuclei appear green and blue; double arrows highlight the approximate direction of the curved groove patterns; scale bars represent 50 μm)

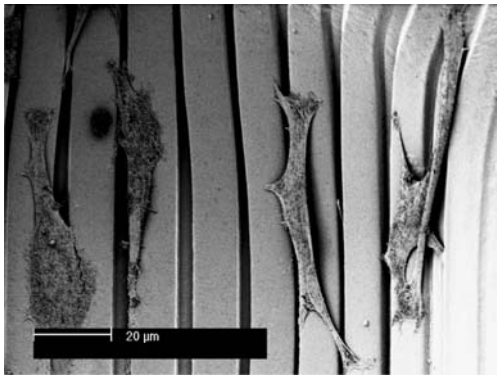

Fig. 12 C2C12 mouse premyoblasts cultured for 2 days on a PLA film with both microgrooves and containers (SEM image; groove width, periodicity and depth prior to thermoforming: 3.5, 15 and 3 µm, respectively)

nuclei were aligned. The corresponding values for the cell bodies should be higher, and therefore similar to our data, as the authors of this study showed in an earlier work with osteoblasts on comparable substrates that cell nuclear alignment provides a conservative or under-estimate of cell body alignment (Charest et al. 2004).

Our results clearly show that contact guidance can also work on highly curved concave surfaces, and that in spite of the surface curvature. In this context, it has to be noted that the guiding topographies in this case, the microgrooves, are curved not only perpendicular to the film plane, together with the film, but also in the film plane to a considerable extent. The ability to align and orient cells via dedicated surface topographies on curved walls of microcontainers offers the possibility to control the organisation of cells inside these artificial environments at least into primitive orders. This can be the organisation or patterning of single cells, monolayers of cells or, depending on the reach of the guidance, possibly even multiple cell layers or cell aggregates (Rivron et al. 2009). Organisation in multiscale hierarchical architectures in turn is a prominent characteristic of tissues *in vivo* where the function of a tissue is intrinsically linked to its 'form' (Ingber 2005). The capacity to organise cells in 3D microconfinements might therefore enable researchers in the near future to drive cells or (micro)tissues *in vitro* towards higher functionality concerning a particular cell-biological or TE application.

4 Conclusions and outlook

We present a technology for the fabrication of 3D substrates in the form of cell container arrays with overlaid surface topographies. The new fabrication technology is based on moulding thin polymer films in two subsequent process steps. Both steps of the simple, fast and cost-effective moulding process can be performed in a conventional heated laboratory press. This enables any cell biology or TE lab to provide itself with cell culture substrates for *in vitro* studies of and in geometrically complex 3D microenvironments. Researchers so far investigating cell-surface-topography interactions on planar substrates from now on can easily extend their research towards curved substrates more accurately reflecting the corresponding situation *in vivo*. Furthermore, due to its nature as a film-based moulding process, the fabrication process has the potential to be scaled up in terms of throughput, for example, if findings from this research shall be transferred to clinical or industrial applications. The two subsequent moulding steps could then be performed as a continuous process based on two-station roller embossing. In such a scenario, in the first station, the film would be topographically patterned, and downstream in the second station, the prepatterned film would be thermoformed to its final 3D shape.

Apart from the above-mentioned biomedical applications, the new technology can promote other applications benefiting from textured 3D surfaces. Topographical micro- and nanopatterns can, for instance, act as superhydrophobic domains in microchannels where they create defined and stable liquid–gas interfaces, or as anti-reflective or self-cleaning layers on miniature lenses.

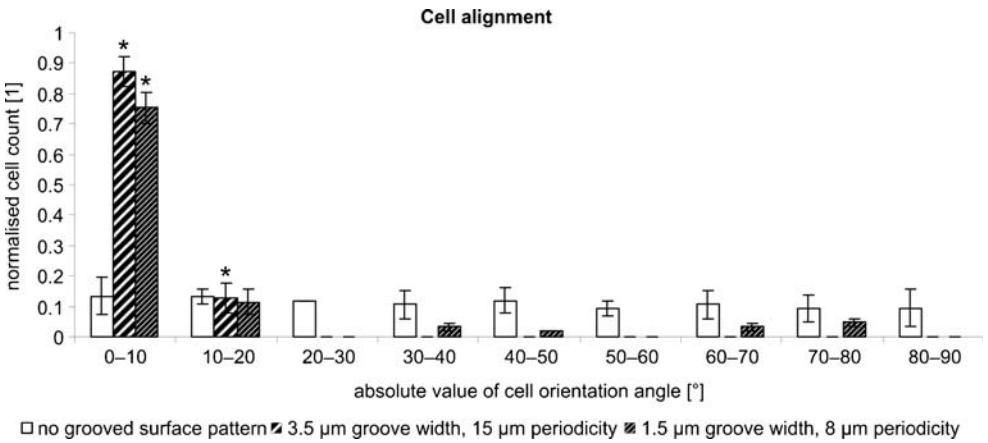

Fig. 13 Cell alignment in film containers with grooved and non-grooved surfaces (orientation angle is the angle with respect to the groove axes; cell count is the count per film sample or well; error bars display standard deviations; asterisks indicate the significance of the corresponding cell count value in an angle range compared to the values in all other angle ranges for a certain film type)

Future work will include a characterisation of resolution and accuracy limits of the new process for the generation of imprint patterns on 3D film substrates, and that also against the background of applying this process as a kind of 3D NIL process. After the cell-biological relevance of substrate curvature could be shown recently by other authors (see also Sanz-Herrera et al. 2009), in this paper, we focused on the technological aspects of substrates, which in addition to their curvature, possess overlaid surface topographies. A detailed, quantitative comparison of such substrates with their planar counterparts concerning the exemplary chosen contact guidance assay is beyond the scope of the present paper, and therefore should be subject of a follow-up article. This also holds true for an in-depth investigation of the underlying mechanisms of contact guidance phenomena on curved substrates.

Acknowledgements R. T., B. P. and D. S. acknowledge the MIRA Institute for Biomedical Technology and Technical Medicine (spearhead project: Advanced Polymeric Microstructures for Tissue Engineering) for financial support. M. E.-M. acknowledges the Nanotechnology network in the Netherlands (NanoNed; project: TMM.7124) for financial support and thanks Prof. Jurriaan Huskens for access to the imprint press.

References

J.L. Charest, L.E. Bryant, A.J. Garcia, W.P. King, Biomaterials **25**, 4767 (2004)
J.L. Charest, A.J. Garcia, W.P. King, Biomaterials **28**, 2202 (2007)
P. Clark, P. Connolly, A.S.G. Curtis, J.A.T. Dow, C.D.W. Wilkinson, Development **99**, 439 (1987)
P. Clark, P. Connolly, A.S.G. Curtis, J.A.T. Dow, C.D.W. Wilkinson, Development **108**, 635 (1990)
A.S.G. Curtis, M. Varde, J Natl Cancer Inst **33**, 15 (1964)
A.S.G. Curtis, P. Clark, Crit Rev Biocompatibility **5**, 343 (1990)
A. Curtis, C. Wilkinson, Biomaterials **18**, 1573 (1997)
R. Flemming, C. Murphy, G. Abrams, S. Goodman, P. Nealy, Biomaterials **20**, 573 (1999)
S. Giselbrecht, T. Gietzelt, E. Gottwald, C. Trautmann, R. Truckenmüller, K.F. Weibezahn, A. Welle, Biomed. Microdevices **8**, 191 (2006)
E. Gottwald, S. Giselbrecht, C. Augspurger, B. Lahni, N. Dambrowsky, R. Truckenmüller, V. Piotter, T. Gietzelt, O. Wendt, W. Pfleging, A. Welle, A. Rolletschek, A.M. Wobus, K.F. Weibezahn, Lab Chip **7**, 777 (2007)
J. Haneveld, Ph.D. Thesis, University of Twente, Enschede, The Netherlands, ISBN 90-365-2312-5 (2006)
V. Hasirci, H. Kenar, Nanomedicine **1**, 73 (2006)
D.E. Ingber, Proc Natl Acad Sci USA **102**, 11571 (2005)
E. Martinez, E. Engel, J.A. Planell, J. Samitier, Ann Anat-Anat Anz **191**, 126 (2009)
B.J. Papenburg, L. Vogelaar, L.A.M. Bolhuis-Versteeg, R.G.H. Lammertink, D. Stamatialis, M. Wessling, Biomaterials **28**, 1998 (2007)
J.Y. Park, D.H. Lee, E.J. Lee, S.H. Lee, Lab Chip **9**, 2043 (2009)
A.F. von Recum, T.G. van Kooten, J Biomater Sci Polym Ed **7**, 181 (1995)
N.C. Rivron, J. Rouwkema, R. Truckenmüller, M. Karperien, J. de Boer, C.A. van Blitterswijk, Biomaterials **30**, 4851 (2009)
A.P. Russo, D. Apoga, N. Dowell, W. Shain, A.M.P. Turner, H.G. Craighead, H.C. Hoch, J.N. Turner, Biomed Microdevices **4**, 277 (2002)
J.A. Sanz-Herrera, P. Moreo, J.M. Garcia-Aznar, M. Doblare, Biomaterials **30**, 6674 (2009)
R. Singhvi, G. Stephanopoulos, D.I.C. Wang, Biotechnol Bioeng **43**, 764 (1994)
J.L. Throne, *Technology of thermoforming* (Hanser, Munich, 1996)
R. Truckenmüller, Z. Rummler, T. Schaller, W.K. Schomburg, J Micromech Microeng **12**, 375 (2002)
R. Truckenmüller, S. Giselbrecht, IEE Proc Nanobiotechnol **151**, 163 (2004)
R. Truckenmüller, S. Giselbrecht, C. van Blitterswijk, N. Dambrowsky, E. Gottwald, T. Mappes, A. Rolletschek, V. Saile, C. Trautmann, K. F. Weibezahn, A. Welle, Lab Chip **8**, 1570 (2008)
X.F. Walboomers, J.A. Jansen, Odontology **89**, 2 (2001)
P. Weiss, Int Rev Cytol **7**, 391 (1958)
F. Zhou, L. Yuan, H. Huang, H. Chen, Chin Sci Bull **54**, 3200 (2009)